

Article

Not peer-reviewed version

---

# Synthesis and Characterization of Hemp Oil-Impregnated Chitosan-Polyvinyl Alcohol Hydrogels for Synergistic Copper (II) Ions Removal from Water

---

[Aryanna Jones](#)<sup>\*</sup> and Kimberly Milligan

Posted Date: 13 May 2026

doi: 10.20944/preprints202605.0853.v1

Keywords: chitosan-PVA; hydrogels; hemp oil; water cleaning; heavy metal remediation



Preprints.org is a free multidisciplinary platform providing preprint service that is dedicated to making early versions of research outputs permanently available and citable. Preprints posted at Preprints.org appear in Web of Science, Crossref, Google Scholar, Scilit, Europe PMC, OpenAlex.

Copyright: This open access article is published under a [Creative Commons CC BY 4.0 license](#), which permit the free download, distribution, and reuse, provided that the author and preprint are cited in any reuse.

Disclaimer/Publisher's Note: The statements, opinions, and data contained in all publications are solely those of the individual author(s) and contributor(s) and not of MDPI and/or the editor(s). MDPI and/or the editor(s) disclaim responsibility for any injury to people or property resulting from any ideas, methods, instructions, or products referred to in the content.

Article

# Synthesis and Characterization of Hemp Oil-Impregnated Chitosan-Polyvinyl Alcohol Hydrogels for Synergistic Copper (II) Ions Removal from Water

Aryanna Jones \* and Kimberly Milligan

Delaware State University

\* Correspondence: ajones202@students.desu.edu

## Abstract

The escalating global crisis of water scarcity, exacerbated by the increasing prevalence of heavy metal contamination from anthropogenic activities, necessitates the development of innovative and sustainable remediation technologies. Recognizing the inherent metal-binding capabilities of *Cannabis sativa* L. (hemp), this study introduces a novel approach for copper(II) ion removal from aqueous solutions. We investigated the synergistic potential of combining hemp-derived cannabinoids with chitosan-polyvinyl alcohol (PVA) hydrogels to create a bio-based adsorbent. Hemp oil, rich in cannabinoids, was incorporated into chitosan-PVA hydrogels synthesized to enhance mechanical stability. The resulting hemp hydrogels (HHGs) were characterized using Fourier Transform Infrared Spectroscopy (FTIR), confirming the integration of the oil within the hydrogel matrix. Inductively Coupled Plasma Mass Spectrometry (ICP-MS) analysis of copper-contaminated solutions treated with HHGs over 24 hours demonstrated a reduction in copper ion concentration, suggesting a biosorption mechanism. Swelling studies revealed an inverse relationship between hemp oil content and water uptake capacity. Thermal studies showed excellent stability amongst gel types. This work establishes the feasibility of utilizing hemp-modified hydrogels as a promising avenue for heavy metal removal, paving the way for future optimization of these bio-composites in both drinking water purification and industrial wastewater treatment applications.

**Keywords:** chitosan-PVA; hydrogels; hemp oil; water cleaning; heavy metal remediation

## 1. Introduction

The increasing global demand for clean water is threatened by widespread contamination, particularly by heavy metals, posing a significant risk to human health and ecosystem stability. Heavy metal pollution, originating from industrial activities, agricultural runoff, and mining operations, persists in aquatic environments due to its non-biodegradable nature, accumulating in food chains and ultimately impacting human populations [2,3]. While effective to some extent, traditional water treatment methods often face limitations in terms of cost-effectiveness, efficiency in removing specific heavy metals, and the generation of secondary pollutants. Therefore, there is an urgent need for the development of new, sustainable, and cost-efficient technologies for heavy metal remediation in water.

In recent years, biosorption has emerged as a promising alternative for heavy metal removal, utilizing materials of biological origin to selectively bind and sequester metal ions from aqueous solutions [9]. *Cannabis sativa* L. (hemp), a versatile plant with a high biomass yield, has demonstrated significant potential in phytoremediation due to its ability to accumulate heavy metals in its tissues [4,25,28]. Furthermore, hemp contains unique bioactive compounds, including cannabinoids, which may contribute to its metal-binding capabilities. Hydrogels, three-dimensional polymeric networks with high water absorption capacity, offer another avenue for water treatment. Chitosan, a natural

polysaccharide, is a particularly attractive hydrogel material due to its biocompatibility, biodegradability, and inherent affinity for pollutants, while polyvinyl alcohol (PVA) can be incorporated to enhance the hydrogel's mechanical strength and stability [23,24]. There is limited research that examines the incorporation of hemp-oil into chitosan/PVA hydrogel networks for copper(II) ion removal from aqueous environments.

This study aims to investigate the potential of combining the advantages of hemp and hydrogels by developing novel hemp hydrogels (HHGs) to remove copper(II) ions from aqueous solutions. Specifically, the study will:

1. Synthesize and characterize chitosan-PVA hydrogels incorporating hemp oil.
2. Assess hydrogel properties.
3. Analyze the structural and chemical properties of HHGs using FTIR spectroscopy.
4. Evaluate the copper(II) ion removal efficiency of HHGs in batch adsorption experiments.

The findings of this research are expected to provide valuable insights into the development of sustainable and effective water treatment technologies for heavy metal remediation, contributing to the mitigation of water pollution and the protection of public health.

## 2. Background

### 2.1. The Critical Importance of Water

Water is an indispensable resource for all life on Earth, underpinning the survival of organisms and the functioning of ecosystems. Beyond its biological necessity, water plays a vital role in human societies, supporting agriculture, industry, transportation, and energy production. The availability of clean water is directly linked to public health, food security, and economic development. However, the increasing global population, coupled with industrial expansion and unsustainable consumption patterns, has placed unprecedented stress on freshwater resources. The *United Nations World Water Development Report 2024* highlights the alarming reality of water scarcity, indicating that half of the global population experiences severe water scarcity for a portion of the year, and a significant number of countries face extremely high-water stress year-round [1]. Approximately 2 million people across the globe lose their life due to water pollution and in lower income countries, chronic conditions are worsened [2]. This scarcity not only threatens human well-being but also amplifies social and political instability. Ensuring access to clean and sustainable water resources is therefore a critical global challenge that demands urgent attention and innovative solutions.

### 2.2. Environmental Pollution and Heavy Metal Contamination

Environmental pollution, driven by factors such as overpopulation, industrialization, and climate change, poses a severe threat to water quality and availability. A major contributor to water pollution is the release of harmful pollutants, including heavy metals, into aquatic ecosystems. Daily, nearly 2 million tons of sewage and wastewater are dumped into water banks across the world and 80% of that in developing countries goes untreated [2]. Heavy metals are metallic elements with a relatively high density that can enter the environment through natural processes like volcanic activity and rock weathering, as well as through anthropogenic activities such as mining, landfills, industrial discharge, and agricultural practices [2]. Unlike many organic pollutants, heavy metals are non-biodegradable, meaning they persist in the environment and can accumulate in sediments, water, and living organisms over time. Smelting, mining, and agricultural repellent sprays contribute significantly to heavy metal contamination in soils that leach into water deposits [3]. This bioaccumulation and biomagnification of heavy metals in the food chain can have severe toxic effects on aquatic life and pose significant risks to human health upon consumption of contaminated water or food.

Examples of heavy metals of particular concern include copper and lead, which are introduced into water systems through various anthropogenic pathways. Inorganic pollutants, such as copper,

are essential micronutrients at low concentrations; they become toxic at elevated levels [4]. Lead, on the other hand, is a non-essential metal with no known biological function and is highly toxic, even at low concentrations [4]. Recently, The U.S. Environmental Protection Agency (EPA) has set a new precedent to remove all lead piping by 2037 to alleviate further contamination [5]. They have established maximum contaminant levels (MCLs) as call-to-action levels for heavy metals in drinking water to protect public health. The EPA has accepted ICP-MS as an analytical tool to accurately quantify trace metals in solution [6]. For copper, the cause of action level is set at 1.3 parts per million [7]. Elevated copper levels within the human body have been linked to kidney damage, cirrhosis of the liver, and gastrointestinal irritation [8]. Additionally, the presence of heavy metals contributes to anxiety, cancer, and reoccurring infections [8]. The persistent nature and toxicity of heavy metals necessitate the development of effective remediation strategies to mitigate their harmful effects on water resources.

### 2.3. Hydrogels as a Promising Technology for Water Treatment

Traditional water treatment methods, including liquid-liquid extraction, ion exchange, and membrane filtration, have been employed to remove heavy metals from contaminated water [9]. However, these methods can be costly, energy-intensive, and may generate secondary pollutants. Adsorption, a process where pollutants adhere to the surface of a solid material (adsorbent), has risen as a cost-effective and efficient alternative for heavy metal removal. Hemp-based felts have been used in this manner to remove copper ions from aqueous solutions through biosorption [9]. In the water treatment sector, nanotechnology has appeared as a promising approach for remediation that could allow local treatment rather than transporting massive amounts of water to centralized treatments centers [10]. Hydrogels, three-dimensional insoluble networks of hydrophilic polymers capable of absorbing large amounts of water, have gained increasing attention in water treatment applications due to their unique properties [11,12]. When loaded with essential oils, these gels uphold their structure and cytocompatibility [12–14]. These properties have made hydrogels popular in the medical industry for drug delivery and topical care [14–16]. Their high-water content, biocompatibility, and tunable structure make them ideal candidates for the removal of various pollutants, including heavy metals [17]. Hydrogels can be synthesized from both natural and synthetic polymers through physical or chemical crosslinking methods, allowing for the design of materials with specific properties tailored to the target pollutant.

Chitosan, a natural polysaccharide, has been extensively investigated for its use in hydrogels for water purification [18]. It is characterized by its molecular weight (MW) and degree of deacetylation (DD), both parameters affecting solubility. Chitosan possesses several advantageous characteristics, including biodegradability, biocompatibility, low-price, non-toxicity, and a high affinity for heavy metals [19–21]. Chitosan is achieved through deacetylating chitin by hydrolysis of its acetamide groups [22]. Its structure is made of repeating linear  $\beta$ -(1,4)-2-amino-D-glucose and  $\beta$ -(1,4)-2-acetamido-D-glucose units that are linked by glycosidic bonds [21]. In chitosan there are more functional amino groups available than its parent polymer, chitin.

The existence of hydroxyl and amino groups in its molecular structure enables chitosan to effectively bind metal ions through electrostatic interactions, hydrogen bonding, and chelation [19,20]. In chelation, metal ions form stable ring complexes with the lone pairs of nitrogen in chitosan's amine groups, locking  $\text{Cu}^{2+}$  ions to the material surface. However, chitosan hydrogels often exhibit limited mechanical strength, which can be improved by incorporating synthetic polymers such as polyvinyl alcohol (PVA).

PVA is a synthetic polymer that is non-toxic, biocompatible, and biodegradable, making it suitable for biomedical and environmental applications [23]. PVA is utilized across industries to formulate films, fibers, and gels [20]. Mean tensile strength and swelling degree in hydrogels has been linked directly to PVA content [24]. Its high density of hydroxyl groups enables extensive intermolecular hydrogen bonding and chain entanglement. These interactions improve the hydrogel's mechanical strength, elasticity, structural integrity, and resistance to dissolution [18]. In

most hydrogel formulations, PVA is more accurately described as a network-strengthening and interfacial stabilizing polymer than as a true surfactant. Chitosan-PVA blends may offer improved performance in water treatment processes, with their efficiency largely influenced by how their networks are formed.

#### 2.4. Physical Crosslinking of CS/PVA Hydrogels

Hydrogels can be formed through various crosslinking methods; this includes physical and chemical crosslinking. Crosslinking will result in changes in elasticity, viscosity, insolubility, and lessen herbal effects. Physical crosslinking, particularly the freeze-thaw method, offers a simple and environmentally friendly approach as it does not require the use of toxic chemical crosslinking agents. The freeze-thaw process involves repeated cycles of freezing and thawing of the polymer solution, leading to the formation of a three-dimensional network structure through non-covalent interactions [24]. During freezing, crystalline zones form through interactions between chitosan and PVA chains. At this time, polymer chains are brought into close proximity, facilitating the formation of inter- and intramolecular hydrogen bonds [24]. Chains then relax during the thawing cycle, allowing movement and new interactions to take place within the hydrogel. In this method, average pore size and swelling properties can be controlled by adjusting the freezing conditions, such as temperature and the number of freeze-thaw cycles [17]. This technique creates structures within their cross-linked fiber networks that can be observed with SEM. Freeze-thaw cycles are immediately followed by freeze drying that evaporates remaining water molecules, resulting in a porous structure.

#### 2.5. Hemp and Heavy Metal Remediation

*Cannabis sativa* L. (hemp) is an economically valuable crop with long traditions of cultivation for its fiber, seeds, and oil dating back to 5000 BC [25, 26]. Hemp has historically been utilized in rope, textiles, and insulation because of the distinct compositions of its stem layers. The bast fibers on the outer stem are flexible and rich in cellulose, whereas the inner woody core contains high lignin concentrations [26, 27]. Recently, hemp has emerged as a promising candidate for phytoremediation, a natural process that utilizes plants' physiological processes to reduce the concentrations of unsafe toxins in water, soil, and sludge [4, 8, 25]. Hemp's rapid growth, metal tolerance, high biomass production, and extensive root systems make it particularly effective in extracting and accumulating heavy metals from soil and water [25,26]. Hemp is also harvested for feedstock, compost, and bioenergy production, while other plants that are considered effective for phytoremediation do not possess valuable applications outside of pollutant uptake [26,28].

Phytoremediation offers a cost-effective and environmentally sustainable approach to remediating contaminated sites, minimizing the need for energy-intensive and disruptive engineering interventions [4, 8]. Hemp's ability to accumulate heavy metals in its tissues, a process known as phytoextraction, has been demonstrated for various metals, including copper and lead [26,28]. Multiple studies record hemp-based biosorbents as effective materials for the adsorption of heavy metals in aqueous solutions [27]. In addition to its phytoremediation capabilities, hemp contains a variety of bioactive compounds, including cannabinoids, which may contribute to its interaction with heavy metals.

The most notable extract from hemp, cannabidiol (CBD), has shown potential in various applications, and their chemical structure suggests they may interact with metal ions. Hemp's sought after characteristics largely contribute to the unique cannabinoids found within their oils. Capturing the active ingredients found within hemp is highly reliant on the extraction method [29]. Besides extraction technique, the part of the plant, temperature, and solvent(s) used will affect the concentrations of bioactive ingredients in the final product [30]. Hemp oil contains triglyceride ester functionalities that give it slightly greater polarity and interfacial compatibility than mineral oil, which is composed primarily of nonpolar hydrocarbons. As a result, hemp oil is often easier to disperse and stabilize in polar hydrogel-based systems, whereas mineral oil behaves as a highly hydrophobic, chemically inert phase with minimal interaction with the gel matrix. Incorporating

hemp-derived oil into hydrogels could create a novel composite material with enhanced heavy metal removal properties, by combining the adsorption capacity of hydrogels with the metal-binding potential of hemp compounds.

### 3. Experimental Design

#### 3.1. Materials

Chitosan powder with a MW of 190-310 kDa was purchased from Sigma-Aldrich (St. Louis, MO, USA). Polyvinyl alcohol (PVA, 98-99% hydrolyzed) was supplied by Thermo Scientific (Waltham, MA, USA). Copper(II) sulfate pentahydrate crystals [CuSO<sub>4</sub>·5H<sub>2</sub>O] were acquired from Alpha Chemicals (Ward Hill, MA, USA). Laboratory-grade acetic acid (CH<sub>3</sub>COOH) and 99.5% ethanol (C<sub>2</sub>H<sub>5</sub>OH) were obtained from Fisher Scientific (Hampton, NH, USA). Deionized (DI) water with a resistivity of 18.2 MΩ·cm was used throughout the experiments. Additional laboratory equipment included a Labconco Freezone 2.5 Plus Freeze dryer (Kansas City, MO, USA), New Brunswick Galaxy 48 S Incubator (Eppendorf AG, Germany), Sartorius Proline Plus pipettes (Göttingen, Germany), and an IKA C-MAG HS 7 magnetic stirring hot plate (Staufen, Germany).

#### 3.2. Hemp Oil Extraction

Hemp biomass (seeds, stems, flowers, and roots) was obtained from Delaware State Agricultural Farm in Smyrna, DE. The plant material was air-dried and then ground using a kitchen blender to increase the surface area for extraction. Forty grams of the blended hemp material was submerged in 400 mL of laboratory-grade ethanol (1:10 w/v ratio) in a 600 mL glass beaker. The mixture was stirred continuously using the IKA C-MAG HS 7 magnetic stirring hot plate at 1200 rpm for 30 minutes at room temperature to facilitate the breakdown of cell walls and the dissolution of cannabinoids into the ethanol. Following extraction, the mixture was filtered through standard coffee filter paper to remove large particulate matter and sediments. The resulting ethanol-cannabinoid solution was transferred to a 400mL beaker and heated on a hot plate at approximately 80°C under a fume hood until all ethanol was evaporated, yielding a cannabinoid-rich hemp oil. The extracted oil was collected and stored in amber glass vials at 4°C until further use.

#### 3.3. Hydrogel Synthesis

Chitosan/PVA hydrogels were synthesized using a freeze-thaw method. Briefly, 0.2 g of chitosan powder was dissolved in 10 mL of 0.1 M acetic acid solution under continuous stirring overnight (approximately 12 hours) at 700 rpm and room temperature to ensure complete dissolution. The next day, 1 g of PVA pellets were dissolved in 10 mL of deionized water by heating the mixture near 80°C under continuous stirring at 300 rpm for 1 hour until clear mixture was obtained. The PVA solution was then allowed to cool to room temperature before combining with the chitosan solution in a 1:1 volume ratio (20 mL total). The mixture was stirred at 800 rpm until a homogenous solution was formed (approximately 30 minutes).

To prepare hemp hydrogels (HHGs), the above procedure was followed, with the addition of 1% (w/w) and 5% (w/w) of the extracted hemp oil to the chitosan/PVA solution. The designated amount of hemp oil was added to the chitosan/PVA mixture under mechanical stirring at 800rpm for thirty minutes. The resulting solutions (control hydrogel - HG, 1% HHG, and 5% HHG) were then poured into separate sterile petri dishes (60 mm x 15 mm) and allowed to degas at room temperature and normal atmospheric pressure for 2 hours.

After degassing, the petri dishes were covered with the appropriate lid and placed in a -20°C freezer for 4 freeze-thaw cycles. Each freeze cycle lasted for 20 hours, followed by thawing at room temperature for 4 hours. After the third freeze-thaw cycle, the hydrogel samples were rinsed three times with deionized water to remove any unreacted monomers or residual acetic acid and then patted dry with Kimwipes. Following the completion of the four freeze-thaw cycles, the hydrogel

samples were lightly wrapped in aluminum foil to protect them from airborne particulates and then freeze-dried using a Labconco Freezezone 2.5 Plus Freeze dryer at  $-80^{\circ}\text{C}$  and a pressure of 0.140 mBar for 48 hours. Three separate batches were prepared for each hydrogel type (HG, 1% HHG, and 5% HHG) to ensure reproducibility. After freeze-drying, the hydrogel samples were removed, cut into 1  $\text{cm}^2$  squares using a sterile scalpel, and labeled accordingly (HG, 1% HHG, and 5% HHG) for subsequent experiments. Figure 1 is a schematic design of the hydrogel synthesis process.

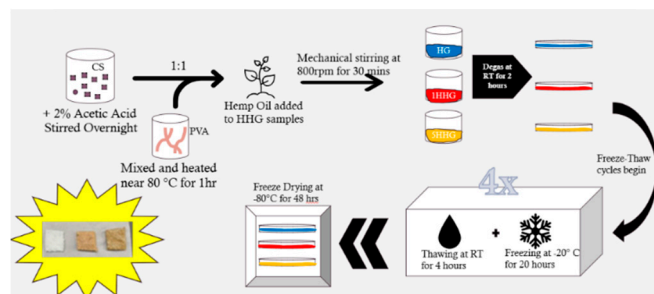


**Figure 1.** Schematic hydrogel synthesis .

### 3.4. Kinetic Studies

A stock solution of copper(II) ions was prepared by dissolving copper(II) sulfate pentahydrate in deionized water to achieve high and low copper concentrations of 1.0 ppm and 0.5 ppm (mg/L). Based on the actual concentration determined by ICP-MS analysis of the stock solution, initial copper(II) ion concentration for the low batch was 0.534 ppm and 1.036 ppm for the high batch. For each kinetic experiment, a pre-weighed, dry hydrogel sample (HG, 1% HHG, or 5% HHG, approximately 0.0222-0.0587g) was placed in one 100 mL beaker containing 40 mL of the 1.036 ppm copper (II) ion solution and another containing 40 mL of the .534 ppm copper(II) ion solution. At predetermined time intervals (1, 3, 6, 12, and 24 hours), each hydrogel sample was carefully removed from the solution, blotted dry with Kimwipes to remove excess surface water, and immediately weighed using an analytical balance with a precision of  $\pm 0.0033\text{g}$ . At each time point, a 1 mL aliquot of the solution was also collected using a sterile pipette and transferred to a sterile microcentrifuge tube. These samples were then acidified with 2% nitric acid to prevent metal precipitation and stored at  $4^{\circ}\text{C}$  until ICP-MS analysis. The kinetic studies were performed in triplicate for each hydrogel type.

### 3.5. Hydrogel Properties

The swelling degree of hydrogels was determined gravimetrically. Pre-weighed, dry hydrogel samples ( $W_0$ ) of each type (HG, 1% HHG, and 5% HHG, approximately 0.0211-0.0732g) were immersed in 50 mL of deionized water and 50 mL solution containing copper(II) ions in separate beakers at room temperature. At the same time intervals as the kinetic studies, the hydrogel samples were removed from the solutions, blotted dry with Kimwipes to remove excess surface water, and weighed ( $W$ ). The swelling degree ( $S$ ) was calculated using the following equation (Eq. 1):

$$S = \frac{W - W_0}{W_0} * 100\%$$

where:

- $S$  is the swelling degree (g/g)
- $W$  is the weight of the swollen hydrogel at a specific time (g)
- $W_0$  is the initial weight of the dry hydrogel (g)

All hydrogel samples will also be put through a small stress test. Thermal degradation analysis of CS/PVA hydrogels is a great tool to assess the thermal stability and composition of polymeric

networks. Typically, thermogravimetric analysis (TGA), is the best tool because it monitors changes in mass affected by temperature. This allows researchers to identify key degradation stages that could include moisture loss, backbone decomposition, and functional group breakdown of their sample. TGA was unavailable, so an alternative method was implemented. Samples from each hydrogel type (HG, 1% HHG, and 5% HHG approximately 13.3442- 13.4695g) were cut at random, placed inside a glass vial, and weighed in grams ( $M_0$ ). The samples were then placed into a New Brunswick 48 S incubator at 50° C for the next five days. Every 24 hours, samples were weighed in the vial and placed back into the incubator until the next measurement ( $M_t$ ). Testing was performed in triplicate ( $n=3$ ). Remaining mass percentage was calculated using the following equation (Eq. 2):

$$\text{Remaining Mass \%} = \frac{M_t}{M_0} \cdot 100$$

where:

- $M_t$  is the mass at a given time (g)
- $M_0$  is the initial mass of the sample (g)

### 3.6. Analysis Techniques

#### 3.6.1. Fourier Transform Infrared Spectroscopy (FTIR)

The structural bonding and chemical composition of the freeze-dried hydrogel samples (HG, 1% HHG, and 5% HHG) were analyzed using an Agilent Cary 630 FTIR spectrometer equipped with an attenuated total reflectance (ATR) accessory. FTIR spectra were recorded in the wavenumber range of 4000-650  $\text{cm}^{-1}$  with a spectral resolution 4  $\text{cm}^{-1}$ . For each sample, 32 scans were collected and averaged, and 32 background scans were performed before each sample analysis. Representative samples from each of the three synthesis batches for each hydrogel type were analyzed to ensure consistency.

#### 3.6.2. Inductively Coupled Plasma Mass Spectrometry (ICP-MS)

The concentration of copper (II) ions remaining in the aqueous solutions after treatment with the hydrogels was determined using an Agilent Technologies 7900 ICP-MS equipped with an S4S Autosampler. Prior to analysis, the collected solution samples were diluted appropriately with 2% nitric acid to fall within the calibration range of the instrument. Calibration curves were prepared using certified standard solutions of copper at concentrations ranging from 1.0-2500 parts per billion (ppb). Values were converted to parts per billion for researchers to calculate with whole numbers [ $1\text{ppm}=1000\text{ppb}$ ]. Quality control measures included the analysis of blanks (deionized water acidified with 2% nitric acid) and certified reference materials (CRMs) to ensure the accuracy and reliability of the measurements. Samples were run in helium mode to minimize polyatomic interferences. Each sample was analyzed in triplicate, and the average concentration and standard deviation were calculated.

#### 3.6.3. Statistical Analysis

All quantitative data were analyzed statistically to determine the significance of observed differences. Data was standardized using the sample mean and standard deviation then plotted against expected normal values to assess linearity for each gel type. Skewness and kurtosis were also evaluated for normality. For data that met the assumption of normality, differences between treatment groups (HG, 1% HHG, and 5% HHG) were analyzed using a two-way analysis of variance (ANOVA) on Microsoft Excel. If necessary, ANOVA was followed by Tukey post hoc tests to identify specific group differences in pairwise comparisons. Statistical significance was defined as a p-value less than 0.05 ( $p < 0.05$ ) for all tests.

## 4. Results and Discussion

### 2.1. CS/PVA Hydrogel Synthesis

Hemp hydrogels (HHGs) were successfully synthesized using the freeze-thaw method, combining chitosan, PVA, and hemp oil. The resulting hydrogel samples were opaque and brittle. After hydration, all the hydrogel samples exhibited flexibility and resistance to breakage, indicating successful crosslinking and formation of a robust network structure. This is because water molecules in the hydrogel matrix permit movement amongst their polymer chains. Water creates free volume space within the network so that the hydrogel can deform and recover. Achieving homogeneity in hydrogels containing hemp oil required greater mixing times and manual labor, suggesting the hydrophobic nature of the oil posed a challenge to its uniform dispersion within the aqueous polymer solution. The use of a sonicator could further enhance homogeneity on their molecular level, leading to improved uniformity of the hemp oil distribution within the hydrogel matrix. Figures 2–4 are SEM images captured of the hydrogel, 1% HHG, and 5% HHG on the surface and cross sections of the materials. These images were captured at an accelerating voltage of 30.00kV, 6.0° C, under 400 Pa of pressure, and a working distance of 4.0±1.0 mm. Formatting for Figures 3–5 is as follows: surface at 500x magnification (top left), surface at 1500x magnification (top right), cross section at 500x magnification (bottom left), and cross section at 1500x magnification (bottom right). The HG shows alignment of the network on the surface and cross sections. Surface alignment decreases in 1% and further in 5% HHG samples. As hemp oil is introduced to the chitosan/PVA blends, spherical pores appear throughout the cross section and expand in size as oil content increases, as previously observed in literature [13].

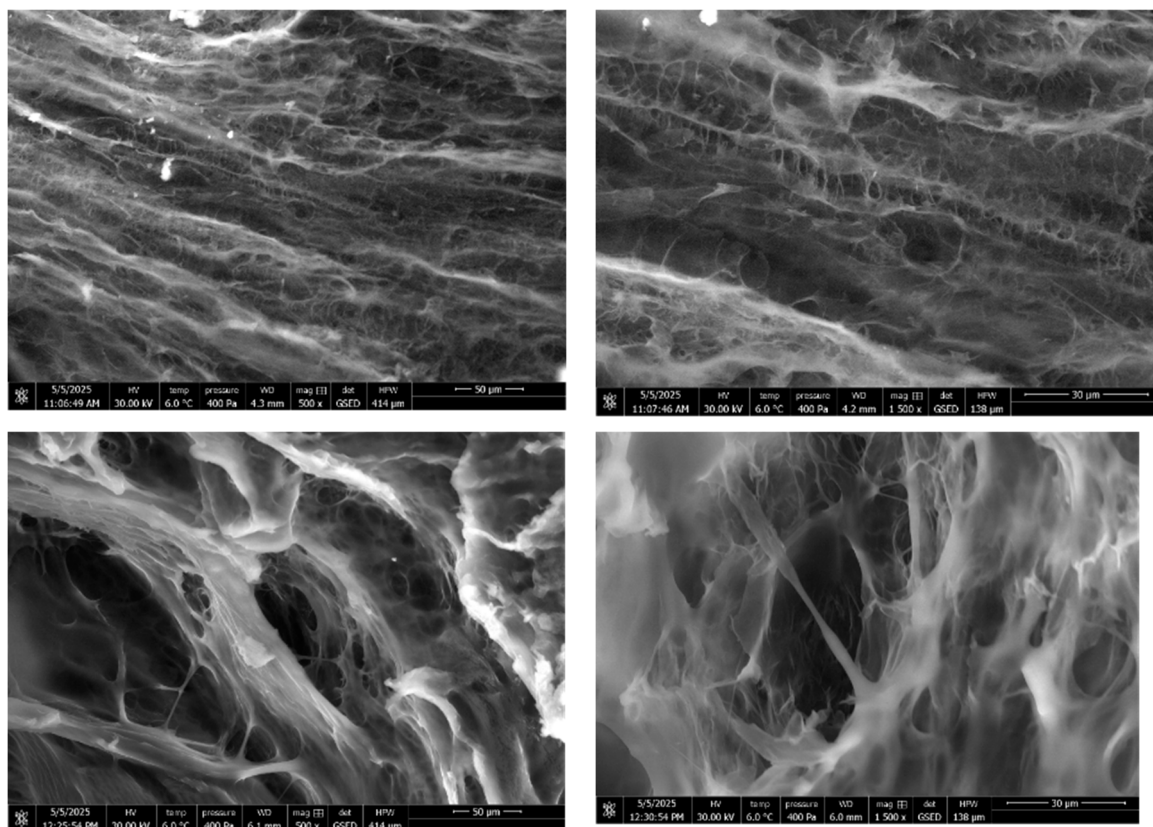


**Figure 2.** SEM Images of the surface and cross sections of hydrogel.

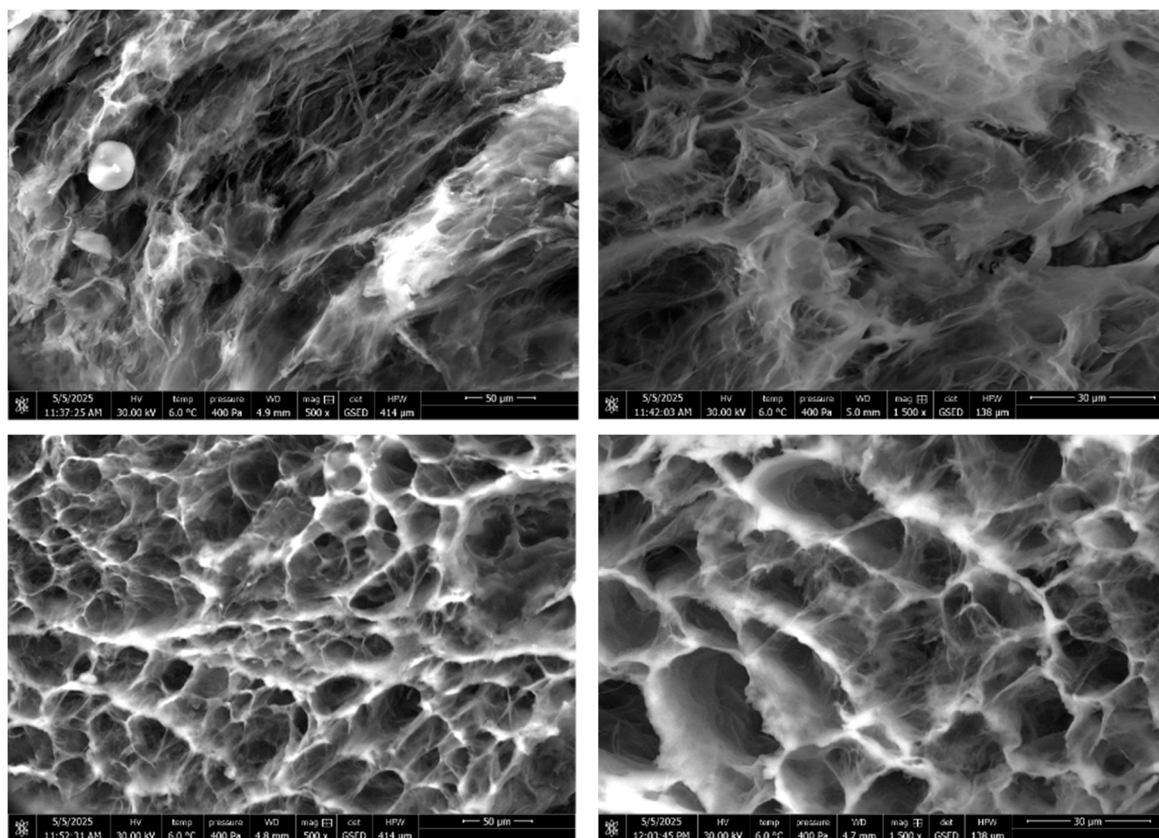


Figure 3. SEM Images of the surface and cross sections of 1% HHG.

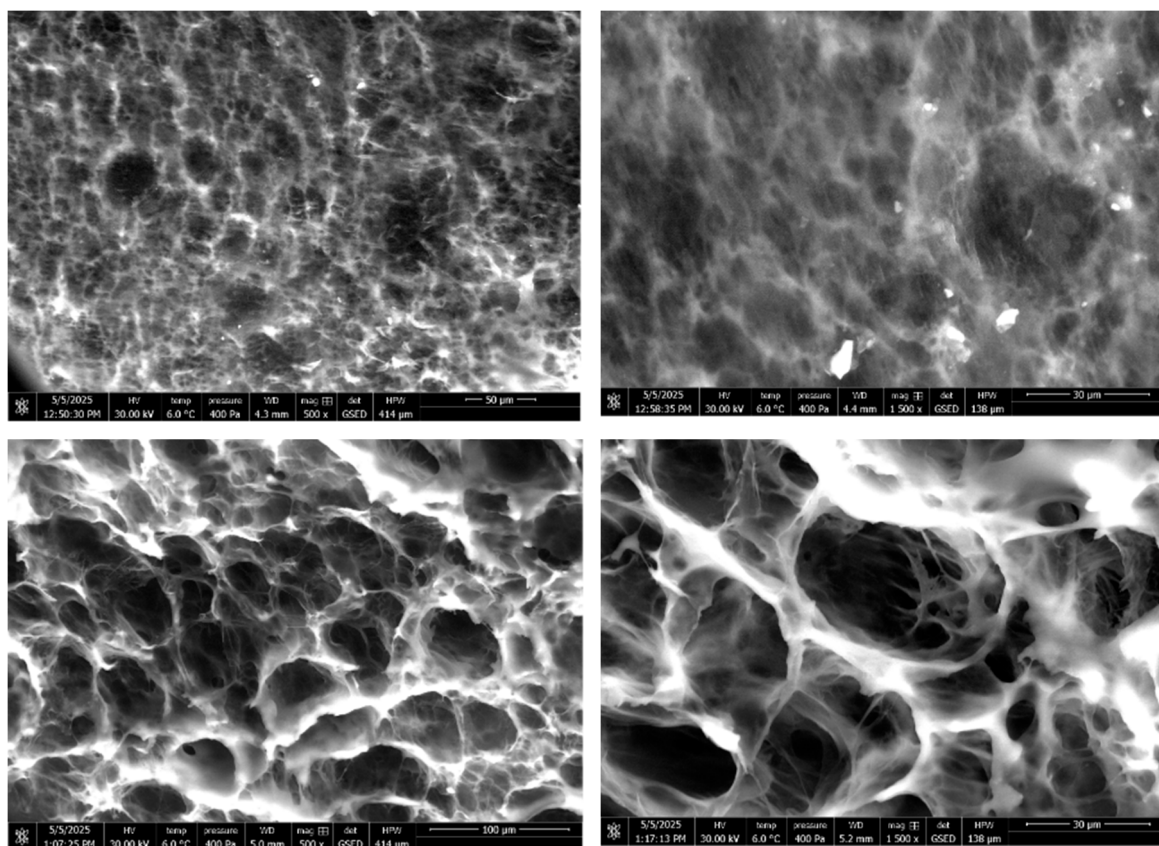
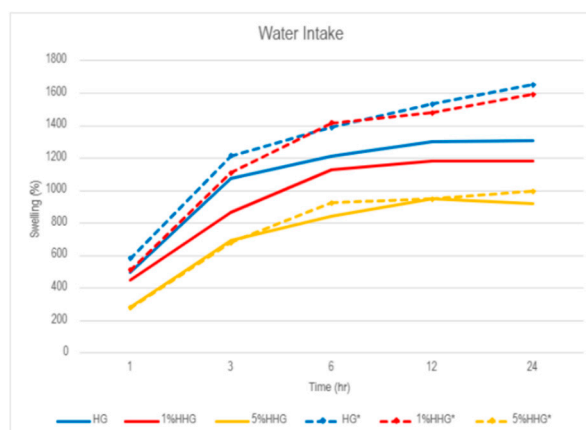


Figure 4. SEM Images of the surface and cross sections of 5% HHG .



**Figure 5.** Swelling percentage graphs of hydrogels in water with (solid line) and without (dotted line)  $\text{Cu}^{2+}$  ions in aqueous solutions. \* Indicates clean water for testing.

## 2.2. Hydrogel Properties

The swelling behavior of hydrogels in aqueous solutions, both with and without copper(II) ions, is illustrated in Figure 6. In both cases, all hydrogel samples exhibited rapid water uptake within the first three hours, demonstrating their high-water absorption capacity. This rapid swelling is attributed to the hydrophilic nature of chitosan and PVA, which facilitates the diffusion of water molecules into the hydrogel network. Additionally, all the samples were still insoluble after 72 hours.

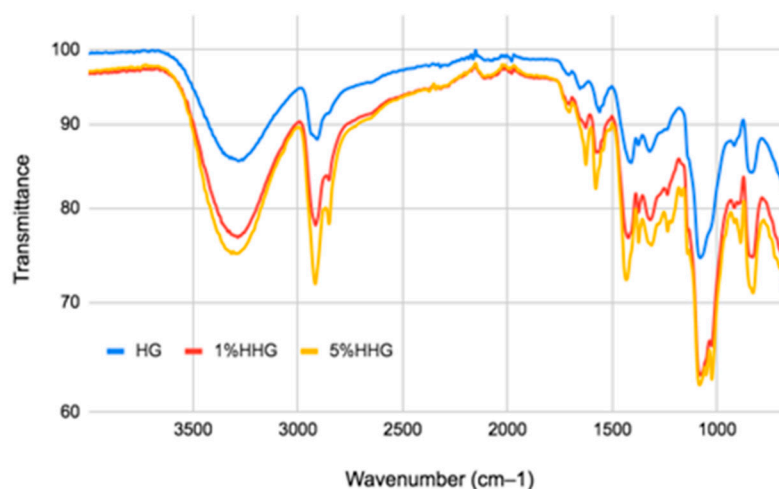


**Figure 6.** Spectra of Hydrogels.

A consistent trend was observed: hydrogels with a higher hemp oil content displayed lower swelling capacities. Specifically, the 5% HHGs exhibited the lowest swelling degree, followed by the 1% HHGs, with the control hydrogels (HG) showing the highest swelling. This inverse relationship between hemp oil content and swelling capacity suggests that the incorporation of hydrophobic hemp oil reduces the overall hydrophilicity of the hydrogel network, hindering water absorption. The oil may occupy space within the network, reducing the available volume for water molecules, or it may interact with the polymer chains, limiting their ability to expand and accommodate water.

Furthermore, the presence of copper(II) ions in the solution lowered the swelling degree of all hydrogel types. The reduced swelling in the presence of copper could be attributed to potential interactions between the copper ions and the hydrogel network, such as ionic crosslinking or coordination, which may lead to a more compact structure and reduced water uptake. Swelling is also driven by osmotic pressure. Water will move throughout the hydrogel to balance the concentration between the surrounding system and the gel. In clean water, there are very few to no

ions available and this large osmotic pressure difference becomes the driving force for water uptake. Figure 5 graphs swelling percentage of each hydrogel type for clean and contaminated water. The x-axis is the duration of time the hydrogel spent in the solution, and the y-axis is the percentage of swelling from the initial dry weight.

Thermal stability of the hydrogels was assessed by monitoring percent mass remaining over a 5-day incubation period at 50 °C. All hydrogel types (HG, 1% HHG, and 5% HHG) demonstrated high mass retention throughout the study, maintaining values above 99%. Mean remaining mass across all days were 99.97±0.0014% for HG, 99.95±0.0359% for 1% HHG, and 99.99±0.0018% for 5% HHG, indicating minimal degradation. At 50 °C, PVA and CS do not thermally degrade so the test operates as a mild thermal stability and dehydration test. Polymer systems remained intact for all hydrogel types. Among these groups, 5% HHG showed the highest mass stability and 1% HHG had the most variability. These results could correspond to what was revealed in the swelling study. 5% HHG demonstrated the lowest swelling capabilities, which aligns with minimal mass loss after exposure to mild heat. The variability in 1% HHG, could be due to heterogeneous oil distribution that could contribute to uneven water loss.

A two-factor ANOVA was conducted to determine the effects of hydrogel type, time, and their interaction on mass retention. The analysis indicated no statistical differences and p values greater than 0.05. These results suggest that neither hydrogel composition or time significantly influenced mass loss at 50 °C. Overall, all formulations exhibited excellent thermal stability, and the incorporation of hemp oil did not result in significant degradation differences compared to the control hydrogel.

**Table 1.** Thermal Degradation ANOVA.

ANOVA			
Source of Variation	F	P-value	F crit
Hydrogel Type	0.845312211	0.439396784	3.315829501
Time	1.474772602	0.234559633	2.689627574
Interaction	0.991373446	0.462370979	2.266163274
Within			

### 2.3. FTIR Analysis

FTIR analysis was conducted on all the samples to ensure the synthesis of a complete hydrogel network and embedding of hemp oil. Seven characteristic signals of chitosan/PVA blends were detected. For the HG with no additives, the broad band at 3280 cm<sup>-1</sup> signifies the stretching vibration mode of PVA hydroxyl groups and 2914 cm<sup>-1</sup> is the stretching vibration mode of their —CH group [11,12]. Transmittance bands for —OH stretching of chitosan are also expected in the 2900-3500 cm<sup>-1</sup> range [17]. Amide groups found in CS structures are identified at 1651 cm<sup>-1</sup>, 1558 cm<sup>-1</sup>, and 1323 cm<sup>-1</sup> for the stretching vibration mode of C=O (amide I), flexion vibration mode of N-H (amide II) and C—N stretching coupled with N-H bending (amide III), respectively [8,12]. The final two signals recognized in PVA are the flexion vibration mode of C-H at 1412 cm<sup>-1</sup> and at 1080 cm<sup>-1</sup>, the stretching vibration mode of C-O groups [12]. Table 2 includes key absorption peaks of the HG from the FTIR spectrum (Figure 6), highlighting characteristic functional groups and their corresponding wavenumbers.

**Table 1.** Absorption Peaks in HG.

Wavenumber (cm <sup>-1</sup> )	Assignment	Associated Structure
3280	—OH	PVA, CS
2914	—CH (stretching)	PVA
1651	Amide I	CS

1558	Amide II	CS
1412	–CH (bending)	PVA
1323	Amide III	Residual acetamide groups of CS
1080	–CO	PVA

FTIR spectra for 1% and 5% HHGs were also analyzed. These hydrogels exhibited all seven characteristics of chitosan and PVA polymers with increased intensity and a few other characteristic peaks due to the presence of implanted hemp oil containing cannabinoid compounds. Compared to 1% HHG, 5% HHG has more intensified peaks because of their greater hemp oil content, seen throughout the entire spectrum. For 1% HHG, the broad band at  $3313\text{ cm}^{-1}$  is the stretching vibration mode of hydroxyl groups in PVA, CS, and cannabinoid phenols [11,12]. This peak is intensified and shifted to  $3339\text{ cm}^{-1}$  for 5% HHG. The rest of the characteristic peaks lined up for 1% and 5% HHG. Again, the stretching vibration mode of –CH assigned to PVA is now identified at  $2918\text{ cm}^{-1}$  due to the addition of fatty acid hydrocarbons [8,11,12]. In the HHG samples, a new peak arises at  $2851\text{ cm}^{-1}$  for the asymmetric stretching aliphatic  $\text{CH}_2$  groups found in cannabinoids [8,11]. This doublet peak confirms hemp oil bonding within the HHGs. Amide I peak is shifted to  $1703\text{ cm}^{-1}$  of the carbonyl presence associated with monoterpenes of cannabinoids. The characteristic peaks of Amide II and III are recognized at  $1576\text{ cm}^{-1}$  and  $1312\text{ cm}^{-1}$ , respectively, due to alkene and methyl group of benzene skeleton vibrations [8,11]. The aromatic benzene ring also affects the flexion vibration mode of C–H at  $1435\text{ cm}^{-1}$ , as peaks between  $1576\text{ cm}^{-1}$  and  $1237\text{ cm}^{-1}$  are often associated with the benzene backbone found cannabinoids [8,11]. The final characteristic band for C–O groups of PVA is slightly shifted to  $1084\text{ cm}^{-1}$  for the inclusion of C–O and C–O–C stretch vibrations particular to hemp oil flavonoids [11]. When comparing all hydrogel types, the drastic intensity at this peak signal's hemp oil bonding in the HHG networks. Table 3 includes key absorption peaks for 1% and 5% HHG, and a full FTIR spectra can be seen in Figure 7. The new peak formed in HHGs at  $2851\text{ cm}^{-1}$  and the intense peaks at  $1084\text{ cm}^{-1}$  confirm hemp oil bonding in the hydrogel matrix. Overall, the FTIR analysis confirms the successful synthesis of chitosan-PVA hydrogels and, importantly, the effective incorporation of cannabinoids from hemp oil into the hydrogel matrix.

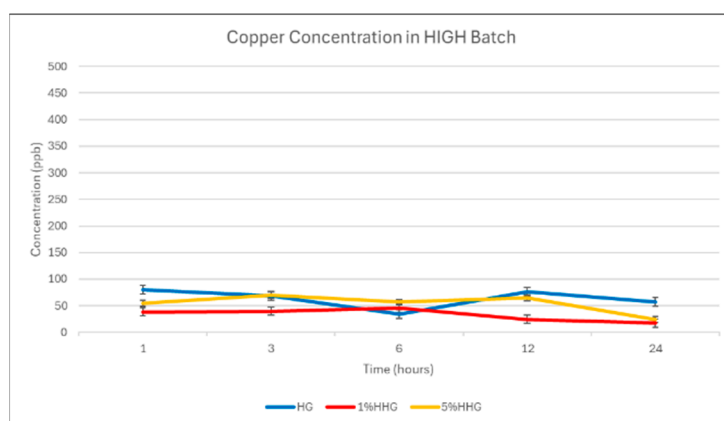


Figure 7.  $\text{Cu}^{2+}$  concentration in high batch.

Table 2. Absorption Peaks in HHG.

Wavenumber ( $\text{cm}^{-1}$ )	Assignment	Associated Structure
3313, 3339	–OH	PVA, CS, and cannabinoid phenols
2918	–CH (stretching)	PVA and hemp fatty acid hydrocarbons
2851	– $\text{CH}_2$	Aliphatic groups of cannabinoids
1703	Amide I and C=C	CS and additional carbonyl groups in cannabinoids
1576	Amide II	CS and cannabinoid benzene backbone
1435	–CH (bending)	PVA

1312	Amide III and CH <sub>3</sub>	Residual acetamide groups of CS and benzene rings of cannabinoids
1084	—CO and C—O—C	PVA and flavonoids from hemp oil

#### 2.4. ICP-MS Results

ICP-MS analysis revealed that the initial copper (II) ion concentration in the prepared solution was 1.036 ppm and 0.534 ppm, close to the intended values. Values were converted to parts per billion so researchers could work with whole numbers. The results demonstrated that the HHGs reduced copper (II) ion concentrations after 24 hours in high and low concentration batches when compared to the control. Data passed normality assumptions before ANOVA tests. In the 1.036 ppm batch, a two-way analysis of variance showed a significant main effect of hydrogel type ( $F(2,30) = 4.67$ ,  $p = 0.017$ ), Tukey's HSD post hoc revealed that 1% HHG had a significantly different mean response than HG, while no significant differences were observed between HG and 5% HHG or between 1% HHG and 5% HHG. In this test, average copper remaining for HG was  $63.43 \pm 8.07$  ppb,  $33.0562 \pm 5.48$  ppb for 1% HHG, and  $30.41 \pm 7.85$  ppb for 5% HHG across all measurements. Figure 7 tracks mean copper concentrations for each gel type in the high concentration batch for 24 hours.

The data set collected from the 0.534 ppm batch shows no statistical significance in ANOVA; hydrogel type  $p = 0.132$ , treatment time  $p = 0.128$ . No post hoc testing was conducted. Figure 8 follows mean copper concentration in this batch over the course of 24 hours.

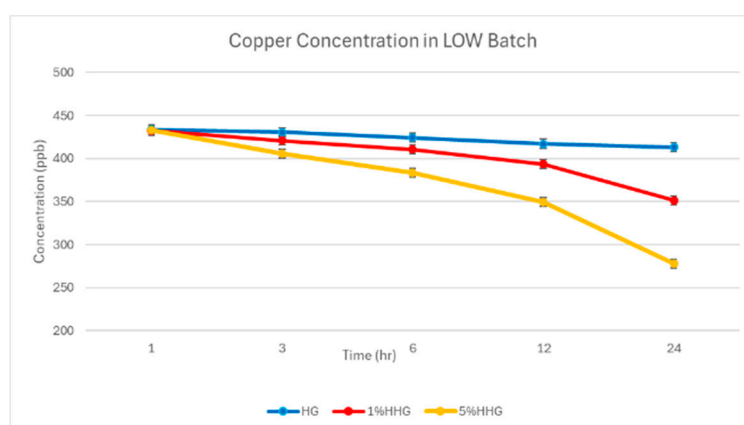


Figure 8. Cu<sup>2+</sup> concentration in low batch.

The fluctuations in copper concentration could be attributed to the dynamic nature of the adsorption process, with copper ions potentially undergoing both adsorption onto the hydrogel surface and desorption back into the solution within this timeframe. When there were more copper ions available in solution, there was a grave difference between initial and final concentrations. This phenomenon is due to the stronger concentration gradient at a higher initial concentration. Based on our theories there would have been more chelation and faster diffusion into pores. Hydrogel uptake was rapid, so increasing the frequency of sampling (e.g., measuring concentrations at shorter time intervals, such as minutes) could provide a more detailed understanding of these early-stage dynamics.

The overall reduction in copper ion concentration suggests that the hemp hydrogels possess some capacity for copper adsorption. However, the extent of removal was not as significant as anticipated, which may be related to the hydrophobic nature of hemp oil and its potential limitations in interacting with hydrophilic metal ions. Enhancing the compatibility between the oil and the aqueous environment, such as through the formation of inclusion complexes, could potentially improve the hydrogels' adsorption capacity.

To further quantify the adsorption behavior of the hydrogels, future studies should employ isotherm models, such as the Langmuir or Freundlich isotherm, to determine the maximum adsorption capacity and calculate the affinity of the hydrogels for copper removal.

### 3. Conclusions

This study successfully demonstrated the feasibility of synthesizing hemp hydrogels (HHGs) for the potential removal of copper(II) ions from aqueous solutions. Chitosan-PVA hydrogels incorporating hemp oil were synthesized using a freeze-thaw method, and the successful incorporation of hemp oil was confirmed by FTIR spectroscopy. Swelling studies revealed an inverse relationship between hemp oil content and water uptake capacity, suggesting that the hydrophobic nature of the oil influences the hydrogel's interaction with water. HHGs showed similar thermal stability to HGs. ICP-MS analysis indicated that HHGs, particularly those with 1% hemp oil content, exhibited some capacity for copper(II) ion removal, although the extent of removal was limited.

The initial objectives of this study were to:

1. Synthesize and characterize chitosan-PVA hydrogels incorporating hemp oil.
2. Assess hydrogel properties.
3. Analyze the structural and chemical properties of HHGs using FTIR spectroscopy.
4. Evaluate the copper(II) ion removal efficiency of HHGs in batch adsorption experiments.

All objectives were successfully addressed. The synthesis and characterization of HHGs were achieved, and the influence of hemp oil on swelling behavior was determined. While some copper(II) ion removal was observed, the results suggest that further optimization of the hydrogel composition and structure is necessary to enhance its adsorption capacity.

The findings of this research contribute to the growing body of knowledge on the use of bio-based materials for water treatment. The combination of hemp's potential for metal binding with the advantageous properties of hydrogels offers a promising avenue for developing sustainable and cost-effective remediation technologies.

**Funding:** This research was funded by DELAWARE SPACE GRANT CONSORTIUM, NASA Grant 80NSSC20M0045.

**Institutional Review Board Statement:** Not applicable.

**Informed Consent Statement:** Not applicable.

**Data Availability Statement:** Data can be recovered at <https://zenodo.org/records/19926590>

**Acknowledgments:** The authors have reviewed and edited the output and take full responsibility for the content of this publication.

**Conflicts of Interest:** The authors declare no conflicts of interest

### Abbreviations

The following abbreviations are used in this manuscript:

CBD	Cannabidiol
CS	Chitosan
HG	Control hydrogel
HHG	Hemp hydrogel
MW	Molecular weight
MCL	Maximum contaminant level
PTSD	Post-traumatic stress disorder
PVA	Polyvinyl alcohol
SEM	Scanning electron microscopy

## References

1. United Nations, The United Nations World Water Development Report 2024: Water for Prosperity and Peace. UNESCO, Paris.
2. Hannah, D. M., Abbott, B. W., Khamis, K., Kelleher, C., Lynch, I., Krause, S., & Ward, A. S. (2022). Illuminating the 'invisible water crisis' to address global water pollution challenges. *Hydrological Processes*, 36(3), Article e14525. <https://doi.org/10.1002/hyp.14525>
3. Sankhla, M. S., Kumari, M., Nandan, M., Kumar, R., & Agrawal, P. (2016). Heavy metals contamination in water and their hazardous effect on human health-A Review. *International Journal of Current Microbiology and Applied Sciences*, 5(10), 759–766. <https://doi.org/10.2139/ssrn.3428216>
4. Husain R, Weeden H, Bogush D, Deguchi M, Soliman M, Potlakayala S, et al. (2019) Enhanced tolerance of industrial hemp (*Cannabis sativa* L.) plants on abandoned mine land soil leads to overexpression of cannabinoids. *PLoS ONE* 14(8): e0221570. <https://doi.org/10.1371/journal.pone.0221570>
5. U.S. Environmental Protection Agency. (2024). *National Primary Drinking Water Regulations for Lead and Copper: Improvements (LCRI)* (Federal Register Doc. No. 2024-23549). *Federal Register*, 89(210), 86418–86666. <https://www.federalregister.gov/d/2024-23549>
6. U.S. Environmental Protection Agency. 1994. "Method 200.8: Determination of Trace Elements in Waters and Wastes by Inductively Coupled Plasma-Mass Spectrometry," Revision 5.4. Cincinnati, OH.
7. Environmental Protection Agency. (n.d.). National Primary Drinking Water Regulations. EPA. <https://www.epa.gov/ground-water-and-drinking-water/national-primary-drinking-water-regulations>
8. Ali, H., Khan, E., & Sajad, M. A. (2013). Phytoremediation of heavy metals—concepts and applications. *Chemosphere*, 91(7), 869–881. <https://doi.org/10.1016/j.chemosphere.2013.01.075>
9. Mongiovi, C., Morin-Crini, N., Lacalamita, D., Bradu, C. et al (2021). Biosorbents from Plant Fibers of Hemp and Flax for Metal Removal: Comparison of Their Biosorption Properties. *Molecules*, 26(14), 4199. <https://doi.org/10.3390/molecules26144199>
10. Amin, M. T., Alazba, A. A., & Manzoor, U. (2014). A review of removal of pollutants from water/wastewater using different types of nanomaterials. *Advances in Materials Science and Engineering*, Article 825910. <https://doi.org/10.1155/2014/825910>
11. Ahmadi, F., Oveisi, Z., Samani, S. M., & Amoozgar, Z. (2015). Chitosan based hydrogels: characteristics and pharmaceutical applications. *Research in Pharmaceutical Sciences*, 10(1), 1–16.
12. Stoleru, E.; Dumitriu, R.P.; Ailiesei, G.-L.; Yilmaz, C.; Brebu, M. Synthesis of Bioactive Materials by In Situ One-Step Direct Loading of *Syzygium aromaticum* Essential Oil into Chitosan-Based Hydrogels. *Gels* 2022,8,225. <https://doi.org/10.3390/gels804022>
13. Chelminiak-Dudkiewicz, D., Smolarkiewicz-Wyczachowski, A., Mylkie, K., Wujak, M., Mlynarczyk, D. T., Nowak, P., Bocian, S., Goslinski, T., & Ziegler-Borowska, M. (2022). Chitosan-based films with cannabis oil as a base material for wound dressing application. *Scientific Reports*, 12(1). <https://doi.org/10.1038/s41598-022-23506-0>
14. Lai, W.-F., & Rogach, A. L. (2017). Hydrogel-Based Materials for Delivery of Herbal Medicines. *ACS Applied Materials & Interfaces*, 9(13), 11309–11320. <https://doi.org/10.1021/acsami.6b16120>
15. Pang, L., Zhu, S., Ma, J., Du et al., (2021). Intranasal temperature-sensitive hydrogels of cannabidiol inclusion complex for the treatment of post-traumatic stress disorder. *Acta Pharmaceutica Sinica B*, 11(7), 2031–2047. <https://doi.org/10.1016/j.apsb.2021.01.014>
16. Zagórska-Dziok, M., Bujak, T., Ziemlewska, A., & Nizioł-Łukaszewska, Z. (2021). Positive effect of cannabis sativa L. Herb extracts on skin cells and assessment of cannabinoid-based Hydrogels Properties. *Molecules*, 26(4), 802–822. <https://doi.org/10.3390/molecules26040802>
17. Figueroa-Pizano, M. D., Vélaz, I., Peñas, F. J., Zavala-Rivera, P., Rosas-Durazo, A. J., Maldonado-Arce, A. D., & Martínez-Barbosa, M. E. (2018). Effect of freeze-thawing conditions for preparation of chitosan-poly (vinyl alcohol) Hydrogels and Drug Release Studies. *Carbohydrate Polymers*, 195, 476–485. <https://doi.org/10.1016/j.carbpol.2018.05.004>

18. Abraham, A., Soloman, P. A., & Rejini, V. O. (2016). Preparation of chitosan-polyvinyl alcohol blends and studies on thermal and mechanical properties. *Procedia Technology*, 24, 741–748. <https://doi.org/10.1016/j.protcy.2016.05.206>
19. Chelu, M., Musuc, A. M., Popa, M., & Calderon Moreno, J. M. (2023). Chitosan hydrogels for water purification applications. *Gels*, 9(8), 664. <https://doi.org/10.3390/gels9080664>
20. Afshar, M., Dini, G., Vaezifar, S., Mehdikhani, M., & Movahedi, B. (2020). Preparation and characterization of sodium alginate/polyvinyl alcohol hydrogel containing drug-loaded chitosan nanoparticles as a drug delivery system. *Journal of Drug Delivery Science and Technology*, 56. <https://doi.org/10.1016/j.jddst.2020.101530>
21. Nicolle, L., Journot, C. M. A., & GerberLemaire, S. (2021). Chitosan functionalization: Covalent and noncovalent interactions and their characterization. *Polymers*, 13(23), 4118. <https://doi.org/10.3390/polym13234118>
22. De Queiroz Antonino, R. S. C. M., Lia Fook, B. R. P., De Oliveira Lima, V. A., De Farias Rached, R. Í., Lima, E. P. N., Da Silva Lima, R. J., Peniche Covas, C. A., & Lia Fook, M. V. (2017). Preparation and characterization of chitosan obtained from shells of shrimp (*Litopenaeus vannamei* Boone). *Marine Drugs*, 15(5), 141. <https://doi.org/10.3390/md15050141>
23. Barbălată-Mândru, M., Serbezeanu, D., Butnaru, M., Rîmbu, C. M., Enache, A. A., & Aflori, M. (2022). Poly(vinyl alcohol)/plant extracts films: Preparation, surface characterization and antibacterial studies against gram positive and gram negative bacteria. *Materials*, 15(7). <https://doi.org/10.3390/ma15072493>
24. Figueroa-Pizano, M., Vélaz, I., & Martínez-Barbosa, M. (2020). A Freeze-Thawing Method to Prepare Chitosan-Poly(vinyl alcohol) Hydrogels Without Crosslinking Agents and Diflunisal Release Studies. *Journal of Visualized Experiments*, (155). <https://doi.org/10.3791/59636-v>
25. Stonehouse, G. C., McCarron, B. J., Guignardi, Z. S., El Mehdawi, A. F., Lima, L. W., Fakra, S. C., & Pilon-Smits, E. A. H. (2020). Selenium Metabolism in Hemp (*Cannabis sativa* L.)—Potential for Phytoremediation and Biofortification. *Environmental Science & Technology*, 54(7), 4221–4230. <https://doi.org/10.1021/acs.est.9b07747>
26. Kumar, S., Singh, R., Kumar, V., Rani, A., & Jain, R. (2017). Cannabis sativa: A plant suitable for phytoremediation and Bioenergy Production. *Phytoremediation Potential of Bioenergy Plants*, 269–285. [https://doi.org/10.1007/978-981-10-3084-0\\_10](https://doi.org/10.1007/978-981-10-3084-0_10)
27. Morin-Crini, N., Loiacono, S., Placet, V., Torri et al., (2018). Hemp-based adsorbents for sequestration of metals: A Review. *Environmental Chemistry Letters*, 17(1), 393–408. <https://doi.org/10.1007/s10311-018-0812-x>
28. Placido, D. F., & Lee, C. C. (2022). Potential of Industrial Hemp for Phytoremediation of Heavy Metals. *Plants*, 11(5), 595. <https://doi.org/10.3390/plants11050595>
29. Devi, V., & Khanam, S. (2019). Comparative study of different extraction processes for hemp (*cannabis sativa*) seed oil considering physical, chemical and industrial-scale economic aspects. *Journal of Cleaner Production*, 207, 645–657. <https://doi.org/10.1016/j.jclepro.2018.10.036>
30. Valizadehderakhshan, M., Shahbazi, A., Kazem-Rostami, M., Todd, M. S., Bhowmik, A., & Wang, L. (2021). Extraction of Cannabinoids from Cannabis sativa L. (Hemp)—Review. *Agriculture*, 11(5), 384. <https://doi.org/10.3390/agriculture11050384>
31. Chetouani, Asma & Elkolli, Meriem & Mahmoud, Bounekhel & Benachour, D.. (2017). Chitosan/oxidized pectin/PVA blend film: mechanical and biological properties. *Polymer Bulletin*. 74. 1-14. [10.1007/s00289-017-1953-y](https://doi.org/10.1007/s00289-017-1953-y).

**Disclaimer/Publisher's Note:** The statements, opinions and data contained in all publications are solely those of the individual author(s) and contributor(s) and not of MDPI and/or the editor(s). MDPI and/or the editor(s) disclaim responsibility for any injury to people or property resulting from any ideas, methods, instructions or products referred to in the content.